

Interface-related damping in polycrystalline Ni₈₁Fe₁₉/Cu/Co₉₃Zr₇ trilayers

S. Zohar and W. E. Bailey

Department of Applied Physics and Applied Mathematics and Materials Science and Engineering, Columbia University, 500 W 120th Street, New York, New York 10027, USA

(Presented 13 November 2008; received 23 September 2008; accepted 17 November 2008; published online 24 February 2009)

We have searched for a signature of nonlocal magnetization dynamics or magnetization dynamics driven by pure spin currents, in magnetically soft polycrystalline Ni₈₁Fe₁₉/Cu/Co₉₃Zr₇ trilayers using ferromagnetic resonance. An interface-related enhancement of damping is expected for each ferromagnetic layer when incorporated in a trilayer; the enhancement should be absent where layer resonances overlap. While size effects in Gilbert damping have been identified, we note that expectations specific to spin pumping are not confirmed. © 2009 American Institute of Physics. [DOI: 10.1063/1.3072030]

“Spin pumping,” the generation of pure spin currents through magnetization precession, is a new idea in magnetization dynamics.¹ In the proposed mechanism, magnetization precession at the broken symmetry of a ferromagnetic/noble metal (FM/NM) interface creates a source for pure spin current ejected into the NM layer. The associated loss of angular momentum in the FM layer manifests itself through an enhanced relaxation rate (damping) acting at the interface.

Spin pumping has been identified in three different forms of interface-related damping in ferromagnetic heterostructures. In all cases, the enhanced damping is predicted to be Gilbert type ($\Delta H \propto \omega$) and inversely dependent on FM layer thickness ($\Delta H \propto 1/t_{\text{FM}}$). First, in structures with a single FM layer, enhanced damping has been attributed to the propagation of spin currents into “spin sink” layers, typically Pt or Pd, which can be in direct contact with the FM layer² or removed through a NM layer.^{3,4} Second, in structures with multiple ferromagnetic layers, such as “spin-valve” type FM₁/NM/FM₂ trilayers, spin current generated at one layer is thought to be absorbed at the opposite layer. For a single layer undergoing ferromagnetic resonance (FMR) precession, this enhances its damping while exerting a small influence on the motion of the opposite layer.⁵ Finally, where the two layers have nearly equal FMR frequencies, a third hallmark is that the motion tends to “lock” in phase and the enhanced damping vanishes.⁶

Magnetization dynamics resulting from spin pumping can be described through additional terms in the Landau Lifshitz Gilbert equation (LLG) (Ref. 7). For FM₁/NM/FM₂ heterostructures, the LLG equation is modified as⁶

$$\dot{\mathbf{m}}_1 = -\gamma_1 \mathbf{m}_1 \times H_{\text{eff},1} + \alpha_1 \mathbf{m}_1 \times \dot{\mathbf{m}}_1 \alpha'_1 (\mathbf{m}_1 \times \dot{\mathbf{m}}_1 - \dot{\mathbf{m}}_2), \quad (1)$$

where the first two terms describe precession and relaxation in the absence of spin pumping, and α'_1 is the spin-pumping damping parameter described by⁶

$$G' = \alpha' \gamma M_S = \frac{g_L^2 \mu_B^2}{2h} \left(\frac{g^{\uparrow\downarrow}}{S} \right) \frac{1}{d}, \quad (2)$$

in cgs units; G' is an additional Gilbert relaxation rate, γ is the gyromagnetic ratio, M_S is the saturation magnetization,

g_L is the Lande- g factor, μ_B is the Bohr magneton, \mathbf{m} is the magnetization divided by the saturation magnetization, and h is Planck's constant. The prefactor evaluates to 28.35 MHz nm³ for the typical case of $g_L=2.09$. The parameter $g_{\text{eff}}^{\uparrow\downarrow}/S$ is the effective mixing conductance per interfacial area; d is the FM layer thickness. When the FM₁ layer is precessing and the FM₂ layer is stationary ($\dot{\mathbf{m}}_2 \approx 0$), the FM₁ layer is subjected to an additional damping of α'_1 . When both FM layers are precessing, the motion is coupled and is treated by solving Eq. (1) for both layers simultaneously; if the motions of \mathbf{m}_1 and \mathbf{m}_2 are equal, the α'_1 goes to zero.⁸

In prior studies, damping from spin sink overlayers has been identified primarily in studies of polycrystalline films, particularly, in Ni₈₁Fe₁₉. Damping in spin-valve systems, on the other hand, has been identified exclusively in epitaxial Fe/Au/Fe on GaAs. It has not yet been shown that polycrystalline spin valves (trilayer structures) exhibit any additional interface-related damping when compared with similar FM layer structures of comparable size.

In this study, we investigate polycrystalline spin valves for the same hallmarks of spin pumping observed in epitaxial spin valves. Four series [(a)–(d)] of samples were deposited for the study. The first two series [(a) and (b)] compare interface-related damping of Ni₈₁Fe₁₉ layers in single films and spin valves: for (a), Ni₈₁Fe₁₉(d)/Cu(3 nm) and for (b), Ni₈₁Fe₁₉(d)/Cu(5 nm)/Co₉₃Zr₇(5 nm)/Cu(3 nm). The second two series [(c) and (d)] compare interface-related damping of Co₉₃Zr₇ layers in single films and spin valves: for (c), Cu(5 nm)/Co₉₃Zr₇(d)/Cu(3 nm) and for (d), Ni₈₁Fe₁₉(5 nm)/Cu(5 nm)/Co₉₃Zr₇(d)/Cu(3 nm).

All layers were deposited by UHV magnetron sputtering, at a base pressure of 3×10^{-9} Torr onto thermally oxidized Si substrates. Pressures immediately prior to deposition were typically 3×10^{-8} Torr; Argon gas pressures were 3.9×10^{-3} Torr during sputtering. Deposition rates were calculated using a quartz crystal balance, which could be positioned removably at the substrate location. Deposition rates were measured as ~ 6 Å/s for Ni₈₁Fe₁₉, ~ 3 Å/s for Co₉₃Zr₇, and ~ 4 Å/s for Cu, with sputtering powers in the range of 250–300 W for Ni₈₁Fe₁₉ and Co₉₃Zr₇ and 100 W for Cu.

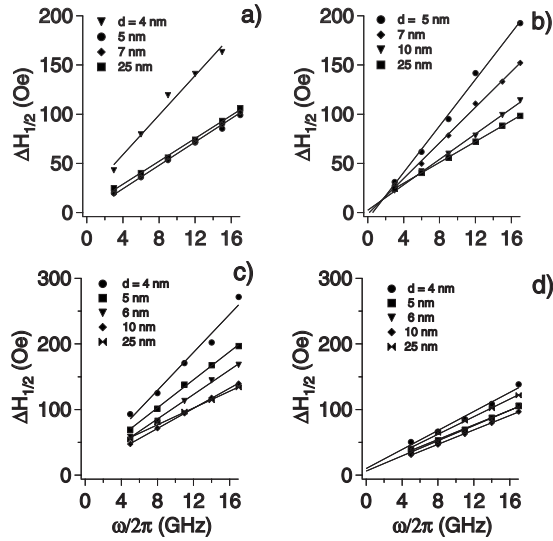


FIG. 1. Linewidths for (a) single $\text{Ni}_{81}\text{Fe}_{19}$ layers (series a), (b) $\text{Ni}_{81}\text{Fe}_{19}$ in spin valves, (c) single $\text{Co}_{93}\text{Zr}_7$ layers, and (d) $\text{Co}_{93}\text{Zr}_7$ in a spin valve.

The Argon pressure has been elevated by $\sim 30\text{--}50\%$ above typical sputtering pressure in these depositions to enhance uniaxial anisotropy of the films. Orthogonal induced anisotropies are formed in the $\text{Ni}_{81}\text{Fe}_{19}$ and $\text{Co}_{93}\text{Zr}_7$ films of ~ 20 Oe and ~ 50 Oe, respectively, roughly along the direction of the deposition flux in the confocal sputtering geometry. This orthogonal induced anisotropy was used to engineer a crossing of the field dependent FMR frequencies $\omega(H)$ between 3.0 and 4.5 GHz, in order to search for the “third” hallmark of spin pumping.

Magnetic properties of the films were investigated by broadband FMR. We measure in-plane (parallel condition) field-swept FMR over a frequency range of 1–18 GHz using a coplanar wave guide to excite rf fields. We fit the single layer FMR line shapes with a dispersion-corrected Lorentzian to extract resonant fields H_{res} and full width half power linewidths $\Delta H_{1/2}$. In the vicinity of the FMR frequency crossing, the FMR line shapes are fit to the sum of two dispersion corrected Lorentzians. When this method does not converge, we fit the data with a single Lorentzian. Gilbert damping constants for each thickness are extracted using variable-frequency FMR linewidth, as $\Delta H_{1/2} = \Delta H_0 + 2\alpha\omega/\gamma$. Effective $4\pi M_S$ values g_L and anisotropy fields were fitting using the Kittel equation $\omega^2 = \gamma^2(H + H_K + 4\pi M_S)(H + H_K)$ valid along the easy and hard axes.

The variable frequency FMR linewidth data for the four series of samples are presented in Fig. 1. The linewidths found are linear in the frequency in all cases with a small inhomogeneous component $\Delta H_0 < 20$ Oe. There is an evident thickness dependence of the slopes in series (b), (c), and (d). The extracted thickness dependence of α is much stronger in series (b) compared with series (a), where we have added the effect of the $\text{Cu}/\text{Co}_{93}\text{Zr}_7$ interface on the $\text{Ni}_{81}\text{Fe}_{19}$ damping. However, in comparing series (c) and (d), we note that the primary effect of adding the $\text{Cu}/\text{Ni}_{81}\text{Fe}_{19}$ interface on the $\text{Co}_{93}\text{Zr}_7$ layer damping is to *reduce* the size effect in damping. While the behavior of $\text{Ni}_{81}\text{Fe}_{19}$ damping is qualitatively consistent with additional damping from the opposite

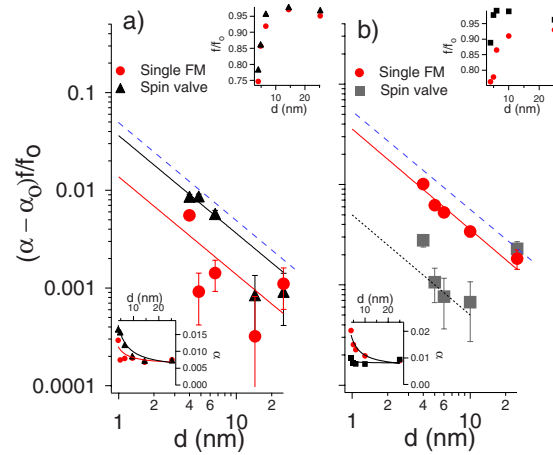


FIG. 2. (Color online) Interface-related damping of comparison of $\text{Ni}_{81}\text{Fe}_{19}$ single layer and spin valve (a) and of $\text{Co}_{93}\text{Zr}_7$ in single layer and spin valve (b). Dashed line: results found for single $\text{Ni}_{81}\text{Fe}_{19}/\text{Pt}$ interfaces (Ref. 4).

$\text{Cu}/\text{Co}_{93}\text{Zr}_7$ interface, the behavior of the $\text{Co}_{93}\text{Zr}_7$ damping cannot be interpreted in this way.

A more quantitative description of the interface-related damping is presented in Fig. 2. Here we plot $(\alpha - \alpha_0)f/f_0$ as a function of thickness d after² where α_0 is the bulk damping, f is the thickness dependent atomic magnetization in μ_B/atom , and f_0 is the corresponding value for bulk films. (f and $4\pi M_S$ are related to good accuracy by $1 \mu_B/\text{atom} \sim 10$ kG.) This form takes into account the increased effectiveness of the torque from pumped spin current on a layer with reduced magnetic moment, as described in Eq. (2). Bulk saturation magnetization values M_S were found to be 10.5 and 16.7 kOe for $\text{Ni}_{81}\text{Fe}_{19}$ and $\text{Co}_{93}\text{Zr}_7$, respectively, which are in good agreement with previously reported bulk values.^{9–11} Bulk damping values α_0 were taken as 0.0067 and 0.007 for $\text{Ni}_{81}\text{Fe}_{19}$ and $\text{Co}_{93}\text{Zr}_7$, respectively, which are in good agreement with bulk values in other investigations.^{9,11} We find the interface-related damping for the $\text{Ni}_{81}\text{Fe}_{19}$ to be $\alpha' = 0.014$ nm/ d in the single layer and $\alpha' = 0.036$ nm/ d in the spin valve for an additional contribution due to the second FM layer of 0.022 nm/ d . The damping enhancement for the $\text{Co}_{93}\text{Zr}_7$ single layer and $\text{Co}_{93}\text{Zr}_7$ spin valve are found to be $\alpha' = 0.036$ nm/ d and $\alpha' = 0.008$ nm/ d , respectively. In this case, any additional damping arising from the second FM layer could be zero, negative, or masked by some other dominant effect.

Our experimental data are plotted together with $\text{Pt}/\text{Ni}_{81}\text{Fe}_{19}(d)/\text{Pt}$ data recorded by Mizukami *et al.*,² which are divided by two to reflect the effect of a single interface, and which have been interpreted previously with a $g^{\uparrow\downarrow}/S = 25.8$ nm⁻².¹ The effect of spin pumping in the Pt spin sink is inferred to be roughly twice as large as any which might be present in the $\text{Ni}_{81}\text{Fe}_{19}$ layers considered here. Note, however, that an interface-related damping of comparable magnitude (0.036 nm/ d) is seen in the single $\text{Co}_{93}\text{Zr}_7$ layer; here no obvious spin sinks are present.

Selected spin valves from series (b) were rotated by 90° aligning $\text{Ni}_{81}\text{Fe}_{19}$ along its easy axis ($H_K \sim 20$ Oe) and $\text{Co}_{93}\text{Zr}_7$ along its hard axis ($H_K \sim -50$ Oe) with respect to the applied field. Because of the larger moment of the

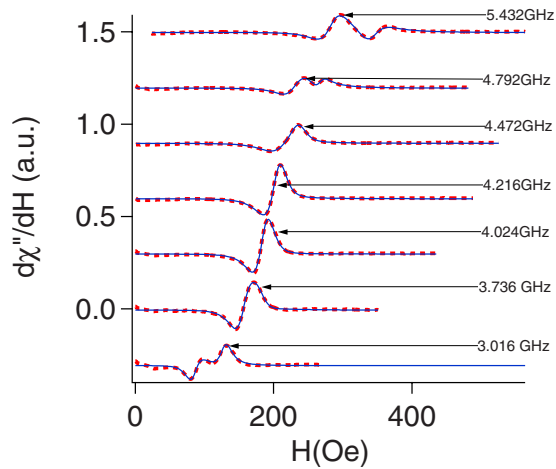


FIG. 3. (Color online) Representative FMR line shapes for $\text{Ni}_{81}\text{Fe}_{19}(5 \text{ nm})/\text{Cu}(5 \text{ nm})/\text{Co}_{93}\text{Zr}(5 \text{ nm})$. The dashed lines represent the data and the unbroken line represents the fit.

$\text{Co}_{93}\text{Zr}_7$ estimated from $\omega(H)$ at $4\pi M_S = 16.7 \text{ kG}$ ($g_L = 2.15$) compared with $4\pi M_S = 10.5 \text{ kG}$ ($g_L = 2.09$) for the $\text{Ni}_{81}\text{Fe}_{19}$, the slope of $\omega(H)$ is expected to be higher for the $\text{Co}_{93}\text{Zr}_7$ than for the $\text{Ni}_{81}\text{Fe}_{19}$ resonance, and the resonance lines will cross between 3.0 and 4.5 GHz, as shown Fig. 4. Ferromagnetic resonance was characterized at small frequency intervals ($\sim 48 \text{ MHz}$) over the range of 2.5–5.5 GHz. Representative line shapes are shown in Fig. 3. For 3.016 GHz, one can see the $\text{Co}_{93}\text{Zr}_7$ line shape at low field and that for $\text{Ni}_{81}\text{Fe}_{19}$ at high field; for 5.432 GHz, the resonance positions are reversed, with $\text{Ni}_{81}\text{Fe}_{19}$ at high field and $\text{Co}_{93}\text{Zr}_7$ at low field. In the range of 4–4.2 GHz, the modes appear as a single FMR absorption.

In Fig. 4, we show the field for resonance and linewidths ($\Delta H_{1/2}$) for the two fitted lines. For each trilayer, the resonance associated with $\text{Cu}/\text{Co}_{93}\text{Zr}_7$ increases more rapidly than that for $\text{Ni}_{81}\text{Fe}_{19}$ and crosses the zero frequency axis at positive field (not shown). While the linewidth fits are noisy and perhaps not unique near the degeneracy, it is clear that the line shapes do not exhibit a single globally reduced linewidth. $\Delta H_{1/2}$ is never significantly less than an extrapolation of the lower linewidth associated with $\text{Ni}_{81}\text{Fe}_{19}$ to the frequency where resonances cross. Taking the inferred value of

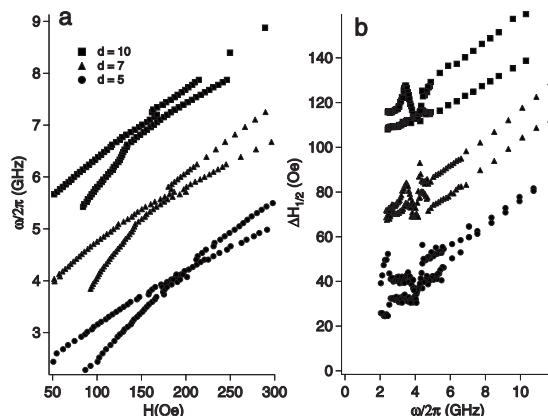


FIG. 4. (a) Resonant field and (b) linewidths for $\text{Ni}_{81}\text{Fe}_{19}(d)/\text{Cu}(5 \text{ nm})/\text{Co}_{93}\text{Zr}_7(5 \text{ nm})$ spin valves. Data has been offset for clarity.

α' for the 5 nm $\text{Ni}_{81}\text{Fe}_{19}$, one expects a linewidth reduction of $\sim 13 \text{ Oe}$, which should be discernible on this scale. Although the higher linewidth resonance line associated with $\text{Co}_{93}\text{Zr}_7$ does appear to exhibit a drop in the region of the crossing, it is not obvious that this drop is above the error introduced from the fitting, as no additional linewidth for $\text{Co}_{93}\text{Zr}_7$ layer has been seen when the linewidths are well separated (Fig. 2).

Our analysis has not accounted for frequency-dependent inhomogeneous broadening due to a distribution in anisotropy field H_k and magnetization $4\pi M_S$. An analysis based on these parameters arises naturally from fixed frequency (e.g., 10 GHz) variable angle measurements of FMR, as carried out in Refs. 4 and 12, and we cannot exclude some contribution to damping from these mechanisms. However, to justify our analysis in terms of Gilbert damping with a fixed inhomogeneous term, we note that our observed linewidth data are accurately linear in frequency for 5 nm films and thicker and reasonably linear for 4 nm films over a substantial frequency range of 2–17 GHz. Inhomogeneous components are less than 10% of intrinsic components at higher frequencies.

In summary, our results point to alternate possible origins of thickness dependent damping in polycrystalline trilayers. While Gilbert type “interface-related” (inverse thickness dependent) damping is clearly seen, the dominant contribution is not clearly related to the addition of a second FM layer, particularly, in the $\text{Co}_{93}\text{Zr}_7$ damping, and does not diminish when the FMR of both layers is excited simultaneously. Thus two important hallmarks of spin pumping are not identified here.

Finally we remark that it is not clear at the time of writing how general the present result may be to polycrystalline trilayers. We cannot rule out at present that some nonideality of the structure prevents the propagation of spin currents in our films alone or perhaps in the use of the $\text{Co}_{93}\text{Zr}_7$ alloy. We note that robust giant magnetoresistive signals have been observed for $\text{Cu}/\text{Co}_{93}\text{Zr}_7$ spin valves in other reports.¹³

We acknowledge the National Science Foundation under Grant No. ECCS-06-22138 and the Army Research Office under Grant No. DAW911NF-07-1-0326 for support.

- ¹Y. Tserkovnyak, A. Brataas, G. Bauer, and B. Halperin, *Rev. Mod. Phys.* **77**, 1375 (2005).
- ²Y. Tserkovnyak, A. Brataas, and G. Bauer, *Phys. Rev. Lett.* **88**, 117601 (2002).
- ³Y. Tserkovnyak, A. Brataas, and G. Bauer, *Phys. Rev. B* **66**, 224403 (2002).
- ⁴S. Mizukami and T. Miyazaki, *Phys. Rev. B* **66**, 104413 (2002).
- ⁵R. Urban, G. Woltersdorf, and B. Heinrich, *Phys. Rev. Lett.* **87**, 217204 (2001).
- ⁶B. Heinrich, Y. Tserkovnyak, A. Brataas, R. Urban, G. Bauer, and G. Woltersdorf, *Phys. Rev. Lett.* **90**, 187601 (2003).
- ⁷L. D. Landau and E. M. Lifshitz, *Phys. Z. Sowjetunion* **8**, 153 (1935).
- ⁸J. Rantschler, P. Chen, A. Arrott, R. McMichael, W. Egelhoff, B. Maranville, and G. Bauer, *J. Appl. Phys.* **97**, 10J113 (2005).
- ⁹Y. Guan and W. E. Bailey, *J. Appl. Phys.* **101**, 09D104 (2007).
- ¹⁰R. C. O’Handley, *Modern Magnetic Materials Principles and Applications*, (Interscience, New York, 2000), p. 189.
- ¹¹J. Beaujour, W. Chen, A. Kent, J. Sun, *J. Appl. Phys.* **99**, 08N503 (2006).
- ¹²D. J. Twisselmann and R. McMichael, *J. Appl. Phys.* **93**, 6903 (2003).
- ¹³M. El Harfaoui, M. Faris, A. Qachaou, J. Ben Youssef, H. Le Gall, and D. Mtalsi, *J. Magn. Magn. Mater.* **223**, 81 (2001).